INVESTIGATION OF HEAT TRANSFER AND VISCOUS DISSIPATION EFFECTS ON THE JEFFERY-HAMEL FLOW OF NANOFLUIDS

by

Amir MORADI [a*], ***Ahmed ALSAEDI*** [b], ***and Tasawar HAYAT*** [b,c]

[a] Young Researchers Club, Arak Branch, Islamic Azad University, Arak, Iran
[b] Department of Mathematics, Quaid-I-Azam University, Islamabad, Pakistan
[c] Department of Mathematics, Faculty of Science, King Abdulaziz University, Jeddah, Saudi Arabia

Original scientific paper
DOI: 10.2298/TSCI120410208M

This article considers the influence of heat transfer on the non-linear Jeffery-Hamel flow problem in a nanofluid. Analysis is performed for three types of nanoparticles namely copper Cu, alumina Al_2O_3, and titania TiO_2 by considering water as a base fluid. The resulting non-linear mathematical problems are solved for both analytic and numerical solutions. Analytic solution is developed by using differential transformation method whereas the numerical solution is presented by Runge-Kutta scheme. A comparative study between the analytical and numerical solutions is made. Dimensionless velocity and temperature, skin friction coefficient and Nusselt number are addressed for the involved pertinent parameters. It is observed that the influence of solid volume fraction of nanoparticles on the heat transfer and fluid flow parameters is more pronounced when compared with three types of nanoparticles. It is also found that skin friction coefficient and Nusselt number for Al_2O_3 nanofluid is highest in comparison to the other two nanoparticles.

Key words: *nanofluid, differential transformation method, numerical solution, Jeffery-Hamel flow*

Introduction

The well known Jeffery-Hamel problem deals with the flow of an incompressible fluid between non-parallel walls. This fundamental problem in viscous fluid is extensively investigated by the various researchers. A survey of early information on this problem can be found in [1, 2]. Apart from using numerical methods in [3, 4], the Jeffery-Hamel flow problem is solved by other techniques such as perturbation method [5], the variation iteration technique, the homotopy perturbation method [6], the Adomain decomposition method [7, 8], the homotopy analysis method [9, 10], and the spectral-homotopy analysis method [11].

At present, there is an increasing interest of the researchers in the analysis of nanofluids. The word nanofluid was introduced by Choi [12]. In fact a nanofluid is a dilute suspension of solid nanoparticles with the average size below 100 nm in a base fluid, such as: water, oil, and ethylene glycol. Nanofluids exhibit thermal properties superior to those of the base fluids of the conventional particle-fluid suspensions [13]. The nanoparticles can be made

* Corresponding author; e-mail: amirmoradi_hs@yahoo.com

of metal, metal oxide, carbide, nitride, and even immiscible nanoscale liquid droplets [14]. Some advantages of nanofluids which make them useful are: a tiny size, along with a large specific surface area, high effective thermal conductivity, and high stability and less clogging and abrasion. The materials with sizes of nanometers possess unique physical and chemical properties [13]. They can flow smoothly through microchannels without clogging them because it is small enough to behave similar to liquid molecules [14]. This fact has attracted many researchers such as Abu-Nada [15], Tiwari and Das [16], Maïga *et al*. [17], Polidari *et al.* [18], Oztop and Abu-Nada [19]. Other than the quoted studies, the literature regarding flows of nanofluids in different configurations is growing rapidly. For example Nield and Kuznetsov [20] provided numerical solution for the effects of Brownian motion thermophoresis in boundary layer flow of viscous nanofluids over a surface embedded in a saturated porous medium. Darcy model is employed. The problem of natural convection flow of nanofluid past a vertical semi-infinite plate is also explored by Kuznetsov and Nield [21]. Nield and Kuznetsov [23] also carried out the numerical investigation for the double-diffusive natural convection boundary layer flow of nanofluid past a vertical plate. Effects of Brownian motion and thermophoresis are taken into account. Analysis of ref. [20] for double-diffusive treatment is presented in study [22]. Laminar forced convection flow of nanofluid in an annulus has been numerically studied by Izadi *et al.* [24]. Single phase approach is employed in the mathematical modeling. Cheng and Minkowcyz [25] considered the free convection flow about a vertical plate embedded in a porous space. Khan and Aziz [26] analyzed the natural convection flow of nanofluid over a plate with a constant heat flux. The Brownian motion and thermophoresis effects are considered and numerical results are presented. Mahmoodi [27] numerically analyzed the free convection flow of nanofluid in a square cavity with an inside heater. Hassani *et al.* [28] carried out the homotpoy analysis method for the problem of boundary layer flow of nanofluid over a linear stretching surface. In this attempt, both the Brownian motion and thermophoresis effects are presented.

Undoubtedly the viscous dissipation yields an appreciable rise in fluid temperature. This is because of the conversion of kinetic motion of fluid to thermal energy and characteristics of source term in the fluid flow. Especially such situation is prominent for fluid flow with heat transfer in microchannels where length-to-diameter ration is very large. Judy *et al*. [29] after conducting experimental study by Tso and Mahulikar [30] concluded that viscous dissipation has a pivotal role in increasing the fluid temperature along the microchannel length for decreasing diameter and increasing fluid velocity. Morini [31] provided a study just to point out the features of viscous dissipation in microchannel flows. It has been declared here that viscous dissipation is important for liquid flows when the hydraulic diameter is less than 100 mm. Das *et al.* [32] explored that the orders of magnitude of nanoparticles are smaller than those of microchannels and thus nanofluids are important for such approximations. Koo and Kleinstreuer [33] numerically discussed the features of viscous dissipation in conduction--convection heat transfer of nanofluid flow. Hady *et al.* [34] considered the viscous dissipation and thermal radiation effects in the flow of viscous nanofluid bounded by a nonlinear stretching surface. The flow of viscous nanofluids over a permeable moving plate in presence of thermal radiation and viscous dissipation is examined by Motsumi and Makinde [35]. Hung [36] provided analytic study for forced convection flow of nanofluids with viscous dissipation. Kuznetsov *et al.* [37] studied the forced convection flow of viscous fluid in a circular duct filled by a saturated porous medium. The walls are at constant temperature. Analysis has been carried out through Brinkman model and longitudinal conduction and viscous dissipation effects. In another attempt, the effects of axial conduction and viscous dissipation are examined foe forced convection flow in a channel by Nield *et al.* [38]. Here the channel walls have constant temperature and Brinkman model is used. Nield *et al.* [39] also investigated the forced convection flow in a channel filled by saturated porous medium when walls hold either at uniform temperature or at uniform heat flux. Here attention is paid to the effects of viscous dissipation and flow work.

In present research, the DTM is applied to find the analytical solutions of non-linear differential problems governing Jeffery-Hamel flow with respect to the heat transfer and viscous dissipation in nanofluids. To our knowledge, the effect of nanoparticles on the characteristics of fluid flow and heat transfer in the Jeffery-Hamel problem is not addressed yet. Hence in this study, the effects of three different types of nanoparticles, namely copper Cu, alumina Al_2O_3, and titania TiO_2 with water as the base fluid are investigated. The dimensionless velocity and temperature, skin friction coefficient and Nusselt number are given proper attention. Numerical and analytical solutions are given and compared.

The concept of differential transformation method was first introduced by Zho [40] in 1986 and it was used for the solutions of linear and nonlinear initial value problems in electric circuit analysis. The main advantage of this method is that it can be applied directly for linear and non-linear differential equation without requiring linearization, discretization, or perturbation. Previously this method is used by various researchers such as Rashidi and Erfani [41] employed the DTM for the solutions of Burger's equation and heat conduction problem in fin with temperature dependent thermal conductivity. Ganji *et al.* [42] used the differential transformation method to determine fin efficiency of convective straight fins with temperature dependent thermal conductivity. Hsiang and Ling [43, 44] presented the new algorithm for the calculations of one and 2-D differential transform of non-linear functions. Jang [45] solved linear and non-linear initial value problems by the projected differential transform method. Rashidi and Erfani [46] used the DTM-Pade for the investigation of MHD stagnation-point flow in porous media with heat transfer. It is noted that when there is an infinite boundary in the problem, the DTM gives the inaccurate results. In this case, by using Pade approximation, the problem can be solved. Complementary information about this method is shown in [47].

Fundamentals of differential transformation method

Consider an analytic function $y(t)$ briefly describes DTM for the convenience of readers. Let us in a domain D with $t = t_i$ showing any point in it. At center t_i, the Taylor series expansion yields [48, 49]:

$$y(t) = \sum_{j=0}^{\infty} \frac{(t-t_i)^j}{j!} \left[\frac{d^j y(t)}{\mathrm{d}t^j} \right]_{t=t_i} \qquad \forall t \in D \tag{1}$$

Maclurin series for $t_\mathrm{i} = 0$ gives:

$$y(t) = \sum_{j=0}^{\infty} \frac{t^j}{j!} \left[\frac{d^j y(t)}{\mathrm{d}t^j} \right]_{t=0} \qquad \forall t \in D \tag{2}$$

By Franco [50] one can write:

$$Y(j) = \sum_{j=0}^{\infty} \frac{H^j}{j!} \left[\frac{d^j y(t)}{\mathrm{d}t^j} \right]_{t=0} \tag{3}$$

in which $y(t)$ shows the original function and $Y(j)$ is the transformed function. The differential spectrum of $Y(j)$ is confined within the interval $t \in [0, H]$, (where H is a constant). The differential inverse transform of $Y(j)$ is given by:

$$y(t) = \sum_{j=0}^{\infty} \left(\frac{t}{H}\right)^j Y(j) \tag{4}$$

Some of the original functions and transformed functions are shown in tab. 1. In fact the concept of differential transformation is Taylor series expansion. For assigned solution the high accuracy may be calculated through more number of series in eq. (4).

Table 1. The fundamental operations of differential transform method

Original function	Transformed function
$f(x) = \alpha g(x) \pm \beta h(x)$	$F(k) = \alpha G(k) \pm \beta H(k)$
$f(x) = g(x)h(x)$	$F(k) = \sum_{i=0}^{k} G(i)H(k-i)$
$f(x) = g(x)^{(n)}$	$F(k) = (k+1)(k+2)\ldots(k+n)G(k+n)$
$f(x) = x^n$	$F(k) = \delta(k-n) = \begin{Bmatrix} 1 & k = n \\ 0 & k \neq n \end{Bmatrix}$
$f(x) = \exp(\alpha x)$	$F(k) = \dfrac{\alpha^k}{k!}$
$f(x) = (1+x)^n$	$F(k) = \dfrac{k(k-1)\ldots(k-m-1)}{k!}$

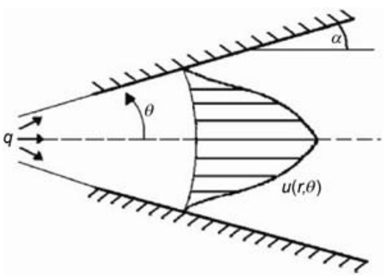

Figure 1. Geometry of the problem

Problem statement

We consider the flow from a source/sink at the intersection between two solid walls that meet at an angle 2α in a water-base nanofluid containing different types of nanoparticles namely Cu, Al_2O_3, and TiO_2 (fig. 1). We choose plane polar coordinates (r, θ) such that the velocity $V[u(r, \theta), 0]$. The equations of continuity, motion, and energy considering viscous dissipation for the problem under consideration give:

$$\frac{\rho_{\mathrm{nf}}\partial}{r\partial r}[ru(r,\theta)] = 0 \tag{5}$$

$$u(r,\theta)\frac{\partial u(r,\theta)}{\partial r} = -\frac{1}{\rho_{\mathrm{nf}}}\frac{\partial p}{\partial r} + \frac{\mu_{\mathrm{nf}}}{\rho_{\mathrm{nf}}}\left[\frac{\partial^2 u(r,\theta)}{\partial r^2} + \frac{1}{r}\frac{\partial u(r,\theta)}{\partial r} + \frac{1}{r^2}\frac{\partial^2 u(r,\theta)}{\partial \theta^2} - \frac{u(r,\theta)}{r^2}\right] \tag{6}$$

$$-\frac{1}{\rho_{\mathrm{nf}} r}\frac{\partial p}{\partial \theta} + \frac{2\mu_{\mathrm{nf}}}{\rho_{\mathrm{nf}} r^2}\frac{\partial u(r,\theta)}{\partial \theta} = 0 \tag{7}$$

$$u(r,\theta)\frac{\partial T(r,\theta)}{\partial r} = \alpha_{\mathrm{nf}}\left(\frac{\partial^2 T(r,\theta)}{\partial r^2} + \frac{1}{r}\frac{\partial T(r,\theta)}{\partial r} + \frac{1}{r^2}\frac{\partial^2 T(r,\theta)}{\partial \theta^2}\right) +$$
$$+\frac{\mu_{\mathrm{nf}}}{(\rho C_p)_{\mathrm{nf}}}\left[4\left(\frac{\partial u(r,\theta)}{\partial r}\right)^2 + \frac{1}{r^2}\left(\frac{\partial u(r,\theta)}{\partial \theta}\right)^2\right] \tag{8}$$

with the subjected boundary conditions *i.e*:
- at the channel centerline: $\partial u(r, \theta)/\partial\theta = 0$, $\partial T/\partial\theta = 0$, $u(r, \theta) = U$
- at the plates, making the body of the channel: $u(r, \theta) = 0$, $T = T_w$.

Here μ_{nf} denotes the viscosity of the nanofluid and ρ_{nf} is the density of the nanofluid. These are expressed by the following definitions:

$$\mu_{nf} = \frac{\mu_f}{(1-\varphi)^{2.5}} \qquad \rho_{nf} = (1-\varphi)\rho_f + \varphi\rho_s \tag{9}$$

where φ depicts the solid volume fraction of the nanofluid, ρ_f – the density of the base fluid, ρ_s – the density of the solid particle, and μ_f – the viscosity of the base fluid. It is worth mentioning that the viscosity of the nanofluid can be approximated as viscosity of a base fluid μ_f containing dilute suspension of fine spherical particles and its expression has been given by Brinkman [51]. Further α_{nf} and k_{nf} are the thermal diffusivity and thermal conductivity of nanofluid, respectively. The value of α_{nf} is [19]:

$$\alpha_{nf} = \frac{k_{nf}}{(\rho C_p)_{nf}}, \quad \frac{k_{nf}}{k_f} = \frac{(k_s + 2k_f) - 2\varphi(k_f - k_s)}{(k_s + 2k_f) + \varphi(k_f - k_s)}$$

$$(\rho C_p)_{nf} = (1-\varphi)(\rho C_p)_f + \varphi(\rho C_p)_s \tag{10}$$

where k_f and k_s are the thermal conductivities of fluid and solid particles, respectively, and $(\rho C_p)_{nf}$ is the heat capacity of the nanofluid.

Equation (5) yields:

$$f(\theta) = ru(r,\theta) \tag{11}$$

Introducing:

$$f(\eta) = \frac{f(\theta)}{f_{max}}, \quad f_{max} = rU, \quad \eta = \frac{\theta}{\alpha}, \quad \xi(\eta) = \frac{T}{T_w} \tag{12}$$

and eliminating p between eqs. (6) and (7), we arrive at:

$$f'''(\eta) + 2\alpha\,\mathrm{Re}\left[(1-\varphi)^{2.5}\left(1-\varphi+\varphi\frac{\rho_s}{\rho_f}\right)\right]f(\eta)f'(\eta) + 4\alpha^2 f'(\eta) = 0 \tag{13}$$

$$\frac{1}{1-\varphi+\varphi\dfrac{(\rho C_p)_s}{(\rho C_p)_f}}\left[\frac{k_{nf}}{k_f}\xi'' + \frac{\mathrm{Pr}\,\mathrm{Ec}}{(1-\varphi)^{2.5}}(4\alpha^2 f^2 + f'^2)\right] = 0 \tag{14}$$

with the following boundary conditions:

$$f(0) = 1, \qquad f'(0) = 0, \qquad f(1) = 0 \tag{15}$$

$$\xi(1) = 1, \qquad \xi'(0) = 0 \tag{16}$$

where the Reynolds number Re, the Eckert number Ec and Prandtl number Pr are expressed as:

$$\mathrm{Re} = \frac{f_{\max}\rho_\mathrm{f}\alpha}{\mu_\mathrm{f}} = \frac{U_{\max} r\rho_\mathrm{f}\alpha}{\mu_\mathrm{f}}\begin{pmatrix}\text{divergent channel}: \alpha > 0, U_{\max} > 0\\ \text{convergent channel}: \alpha < 0, U_{\max} < 0\end{pmatrix},$$

$$\mathrm{Pr} = \frac{\mu_\mathrm{f}(c_p)_\mathrm{f}}{k_\mathrm{f}}, \quad \mathrm{Ec} = \frac{U^2}{(c_p)_\mathrm{f} T_\mathrm{w}} \tag{17}$$

Expressions of skin friction coefficient (c_f) and shear stress (τ_w) are:

$$c_\mathrm{f} = \frac{\tau_\mathrm{w}}{\rho_\mathrm{f} U_{\max}^2} \tag{18}$$

$$\tau_\mathrm{w} = \mu_\mathrm{nf}\left[\frac{1}{r}\frac{\partial u(r,\theta)}{\partial\theta}\right] \tag{19}$$

Substitution of eq. (12) into eqs. (18) and (19) gives:

$$c_\mathrm{f} = \frac{1}{\mathrm{Re}(1-\varphi)^{2.5}} f'(1) \tag{20}$$

The local Nusselt number Nu and heat transfer rate are:

$$\mathrm{Nu} = \frac{r q_\mathrm{w}\big|_{\theta=\alpha}}{k_\mathrm{f} T_\mathrm{w}}, \quad q_\mathrm{w} = -k_\mathrm{nf}\nabla T \tag{21}$$

This expressions in view of eq. (12) yield:

$$\mathrm{Nu} = -\frac{1}{\alpha}\frac{k_\mathrm{nf}}{k_\mathrm{f}}\xi'(1) \tag{22}$$

Solution by differential transformation method

From eqs. (13) and (14) we can write:

$$(k+1)(k+2)(k+3)F(k+3) + 2\alpha\,\mathrm{Re}\left[(1-\varphi)^{2.5}\left(1-\varphi+\varphi\frac{\rho_\mathrm{s}}{\rho_\mathrm{f}}\right)\right]\cdot$$
$$\cdot\sum_{i=0}^{k}(k-i+1)F(i)F(k-i+1) + 4\alpha^2(k+1)F(k+1) = 0 \tag{23}$$

$$\frac{k_\mathrm{nf}}{k_\mathrm{f}}(k+1)(k+2)\Theta(k+2) +$$
$$+\frac{\mathrm{Pr\,Ec}}{(1-\varphi)^{2.5}}\left(4\alpha^2\sum_{i=0}^{k}F(i)F(k-i) + \sum_{i=0}^{k}(i+1)(k-i+1)F(i+1)F(k-i+1)\right) = 0 \tag{24}$$

where $F(k)$ and $\Theta(k)$ are transformed functions of $f(\eta)$ and $\xi(\eta)$, respectively. Now the transformed boundary conditions are given by:

$$F(0) = 1 \quad F(1) = 0 \quad \Theta(1) = 0, \tag{25}$$

$$\sum_{i=0}^{\infty}F(i) = 0, \quad \sum_{i=0}^{\infty}\Theta(i) = 1 \tag{26}$$

Letting $F(2) = \delta$ and $\Theta(0) = \beta$ and invoking eqs. (23) and (24), the other values of $F(k)$ and $\theta(k)$ when $\varphi = 0$ are computed. These are:

$$\begin{aligned}
&F(3)=0\\
&F(4)=-\frac{1}{6}\alpha\delta(\mathrm{Re}+2\alpha)\\
&F(5)=0\\
&F(6)=\frac{1}{90}\alpha\delta(\mathrm{Re}^2\alpha+4\,\mathrm{Re}\,\alpha^2+4\alpha^3-3\,\mathrm{Re}\,\delta)\\
&F(7)=0\\
&F(8)=-\frac{1}{2520}\alpha^2\delta(\mathrm{Re}+2\alpha)(\mathrm{Re}^2\alpha+4\,\mathrm{Re}\,\alpha^2+4\alpha^3-18\,\mathrm{Re}\,\delta)\\
&\vdots
\end{aligned} \tag{27}$$

$$\begin{aligned}
&\Theta(2)=-2\alpha^2\,\mathrm{Pr}\ \mathrm{Ec}\\
&\Theta(3)=0\\
&\Theta(4)=-\frac{1}{3}\mathrm{Pr}\,\mathrm{Ec}\,\delta(2\alpha^2+\delta)\\
&\Theta(5)=0\\
&\Theta(6)=-\frac{1}{90}\mathrm{Pr}\,\mathrm{Ec}\,\delta(-8\alpha^4-4\alpha^3\,\mathrm{Re}-4\alpha^2\delta-8\alpha\delta\,\mathrm{Re})\\
&\Theta(7)=0\\
&\vdots
\end{aligned} \tag{28}$$

Since the above process is continuous, hence putting eqs. (27) and (28) in the main equation based on DTM with $H = 1$, the resulting expressions are:

$$f(\eta)=1+\delta\eta^2-\frac{1}{6}\alpha\delta(\mathrm{Re}+2\alpha)\eta^4+\frac{1}{90}\alpha\delta(\mathrm{Re}^2\alpha+4\,\mathrm{Re}\,\alpha^2+4\alpha^3-3\,\mathrm{Re}\,\delta)\eta^6+\ldots \tag{29}$$

$$\begin{aligned}
\xi(\eta)&=\beta-2\alpha^2\,\mathrm{Pr}\ \mathrm{Ec}\,\eta^2-\frac{1}{3}\mathrm{Pr}\,\mathrm{Ec}\,\delta(2\alpha^2+\delta)\eta^4-\\
&-\frac{1}{90}\mathrm{Pr}\,\mathrm{Ec}\,\delta(-8\alpha^4-4\alpha^3\,\mathrm{Re}-4\alpha^2\delta-8\alpha\delta\,\mathrm{Re})\eta^6+\ldots
\end{aligned} \tag{30}$$

In order to determine δ and β we substitute eq. (26) into eqs. (29) and (30):

$$f(1)=1+\delta-\frac{1}{6}\alpha\delta(\mathrm{Re}+2\alpha)+\frac{1}{90}\alpha\delta(\mathrm{Re}^2\alpha+4\,\mathrm{Re}\,\alpha^2+4\alpha^3-3\,\mathrm{Re}\,\delta)+\ldots=0 \tag{31}$$

$$\begin{aligned}
\xi(1)&=\beta-2\alpha^2\,\mathrm{Pr}\ \mathrm{Ec}-\frac{1}{3}\mathrm{Pr}\,\mathrm{Ec}\,\delta(2\alpha^2+\delta)\\
&-\frac{1}{90}\mathrm{Pr}\,\mathrm{Ec}\,\delta(-8\alpha^4-4\alpha^3\,\mathrm{Re}-4\alpha^2\delta-8\alpha\delta\,\mathrm{Re})+\ldots=1
\end{aligned} \tag{32}$$

From this four equations, we have the desired expressions of $f(\eta)$ and $\xi(\eta)$.

Results and discussion

The non-linear differential problems consisting of eqs. (13) and (14) along with the boundary conditions eqs. (15) and (16) have been solved analytically and numerically by employing DTM and fourth-order Runge-Kutta method, respectively. We carry out the analysis for three different types of nanoparticles namely Cu, Al_2O_3, and TiO_2 with water as the base fluid. The thermophysical properties of different nanoparticles are shown in tab. 2. The comparison between present and other reported results [11, 52] for Re = 50, α = 5°and φ = 0 is shown in tab. 3. It is evident from tab. 3 that the DTM results are in an excellent agreement with OHAM and SHAM results. Effect of solid volume fraction on the dimensionless velocity for Cu, Al_2O_3, and TiO_2 of nanoparticles (when Re = 50 and α = 5°) is displayed in figs. 2-4, respectively. Figure 2 displays that in divergent channel, $f(\eta)$ decreases when the solid volume fraction increases for Cu nanoparticles. It is worth mentioning to point out that the velocity increases when the solid volume fraction increases for Al_2O_3 and TiO_2 nanoparticles (see figs. 3 and 4). It is concluded that the impact of solid volume fraction in Cu-water nanofluid is more evident than the other nanoparticles. Further, it is noticed form figs. 2-4 that there is well agreement between the DTM and numerical results.

Table 2. The physical properties of nanofluids and base fluid [19]

Physical properties	Water (base fluid)	Cu	Al_2O_3	TiO_2
ρ [kgm^{-3}]	977.1	8933	3970	4250
C_p [Jkg^{-1}K^{-1}]	4179	385	765	686.2
k [Wm^{-1}K^{-1}]	0.613	400	40	8.9538

Table 3. Comparison of DTM, OHAM, SHAM and numerical solutions for Newtonian fluid (φ = 0), Re = 50 and α = 5°

η	DTM	OHAM [52]	SHAM [11]	Numerical
0	1	1	1	1
0.1	0.982431	0.98251808	0.982431	0.982431
0.2	0.931226	0.93156588	0.931226	0.931226
0.3	0.850611	0.8513815	0.850611	0.850611
0.4	0.746791	0.74826039	0.746791	0.746792
0.5	0.626948	0.62953865	0.626848	0.6268488
0.6	0.498234	0.50242894	0.498234	0.498234
0.7	0.366966	0.37293383	0.366966	0.366966
0.8	0.238124	0.24508197	0.238124	0.238124
0.9	0.115152	0.1207156	0.115152	0.115152
1	–0.00000021	0.000000001	0	0

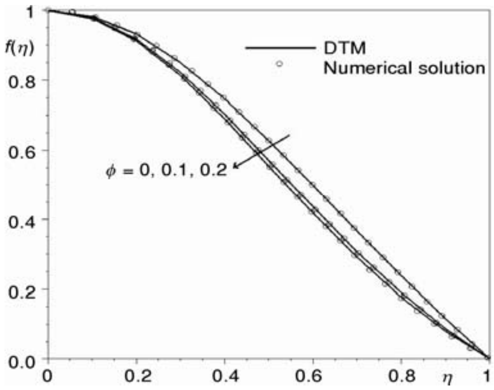

Figure 2. Variation of $f(\eta)$ with different values of solid volume fraction for water-Cu nanofluid when Re = 50 and α = 5

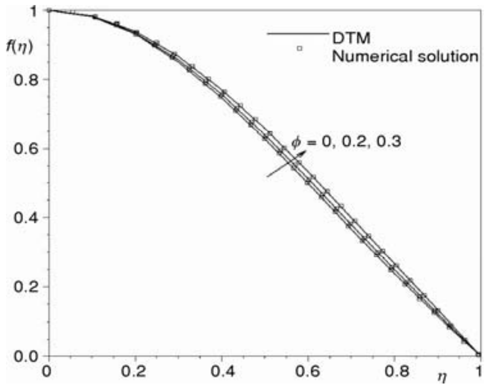

Figure 3. Variation of $f(\eta)$ with different values of solid volume fraction for water-Al_2O_3 nanofluid when Re = 50 and α = 5

Figure 5 shows the changes in the considered nanoparticles on the dimensionless velocity when Re = 80, α = 3°, and φ = 0.2. It is found that the dimensionless velocities for Al_2O_3 and TiO_2 nanoparticles are almost same. It is noticed that values of velocities for Al_2O_3 and TiO_2 nanoparticles are larger than Cu nanoparticle velocity. The effect of solid volume fraction on the dimensionless temperature profile for water-Cu nanoparticle (when Re = 50, α = 5°, and Ec = 0.5) is depicted in fig. 6. It is observed that the temperature increases when the solid volume fraction increases. In all results of this paper, Pr = 6.2 is considered for solution. Figure 7

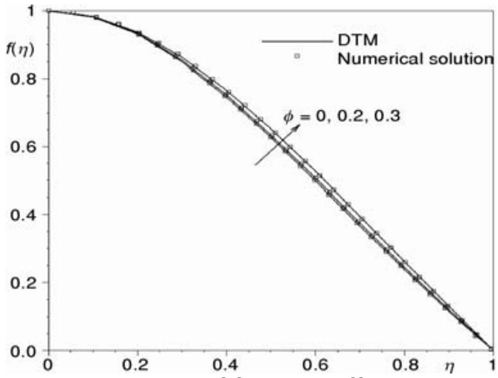

Figure 4. Variation of $f(\eta)$ with different values of solid volume fraction for water-TiO_2 nanofluid when Re = 50 and α = 5

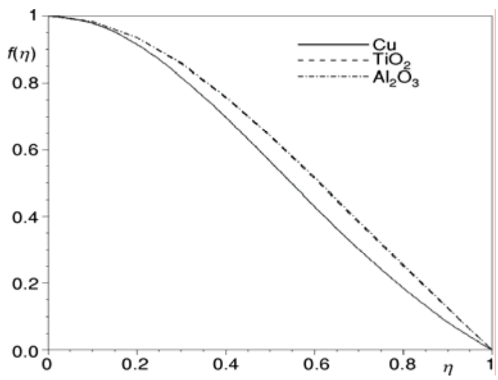

Figure 5. Variation of $f(\eta)$ for three types of nanoparticles when Re = 80, α = 3, and φ = 0.2

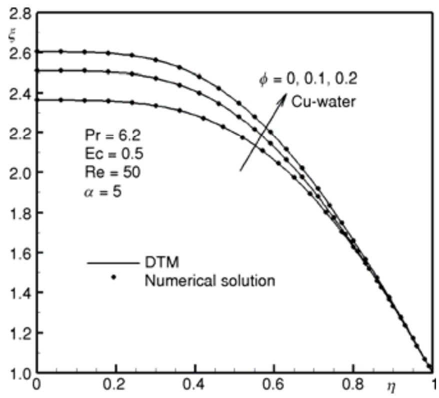

Figure 6. Variation of $\xi(\eta)$ with different values of solid volume fraction for water-Cu nanofluid when Re = 50, Ec = 0.5, and α = 5

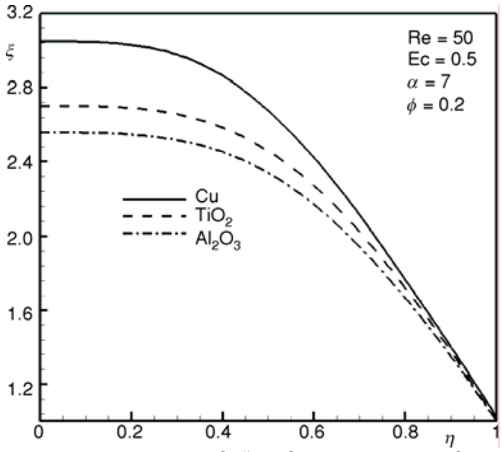

Figure 7. Variation of $\xi(\eta)$ for three types of nanoparticles when Re = 50, α = 7, Ec = 0.5, and φ = 0.2

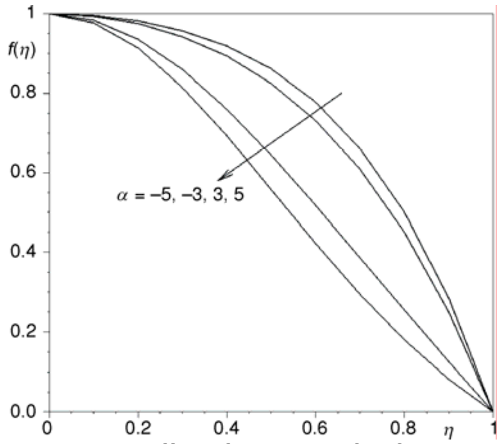

Figure 8. The effect of angle α on $f(\eta)$ for water-Al_2O_3 nanofluid when φ = 0.2, and Re = 50

provide the dimensionless temperature profile for different nanoparticles when other parameters kept fixed at Re = 50, α = 7, Ec = 0.5, and φ = 0.2. It is clear from fig. 7 that Cu nanoparticle has a higher temperature than the other nanoparticles. Figure 8 depicts the velocity profiles for water-Al_2O_3 nanofluid when the angle α is equal to –5, –3, 3, and 5, and other parameters kept fixed at φ = 0.2 and Re = 50. This figure illustrates that in divergent channel, the dimensionless velocity is decreasing function of α. However the dimensionless velocity increases when α is increased in convergent channel. The effect of angle α on the dimensionless temperature for water-Al_2O_3 nanofluid when φ = 0.2 and Re = 50 is shown in fig. 9. This figure describes that the temperature is increasing function of α in divergent channel. Figure 10 explains the dimensionless velocity for water-TiO_2 nanofluid when the Reynolds number Re varies and the other parameters kept fixed at $\alpha = -3$ and $\varphi = 0.1$. It is revealed that in divergent channel, $f(\eta)$ is increasing function of Reynolds number (see fig. 10).

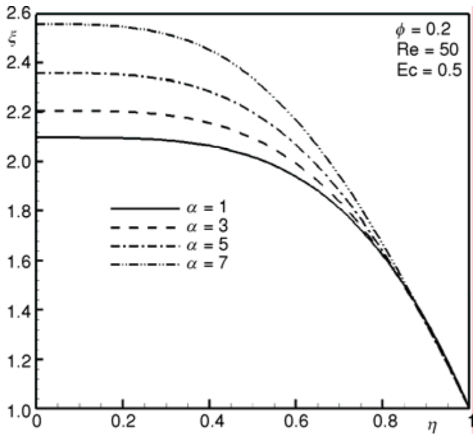

Figure 9. The effect of angle α on $\xi(\eta)$ for water-Al_2O_3 nanofluid when φ = 0.2, Ec = 0.5, and Re = 50

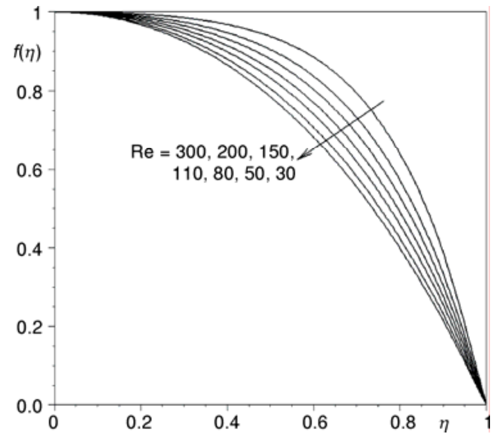

Figure 10. The effect of Reynolds number on $f(\eta)$ for water-TiO_2 nanofluid when α = –3 and φ = 0.1

The impact of Reynolds number Re on the dimensionless temperature $\xi(\eta)$ considering water-TiO_2 nanofluid when remaining parameters kept fixed at α = 3, φ = 0.2, and Ec = = 0.5 is displayed in fig. 11. As shown, an increase in the temperature is found with increased the value of Re. Figure 12 shows the temperature distribution for water-Cu nanoparticles when the Eckert number is allowed to varies and the other parameters fixed at α = –3, Re = = 30, and φ = 0.2. It can be clearly seen that the temperature increases when the value of Ec becomes larger.

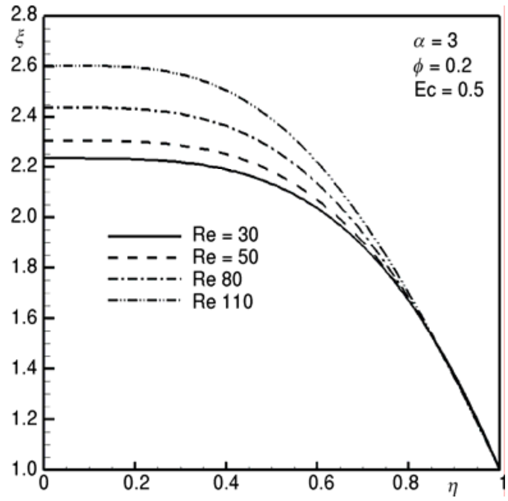

Figure 11. The effect of Reynolds number Re on $\varphi(\eta)$ for water-TiO_2 nanofluid when α = 3, Ec = 0.5 and φ = 0.2

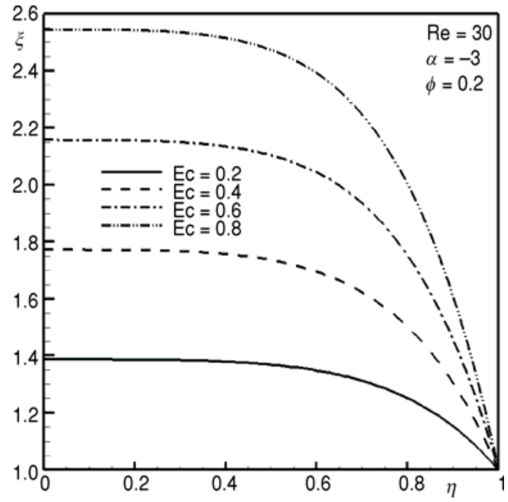

Figure 12. The effect of Eckert number Ec on $\xi(\eta)$ for water-Cu nanofluid when a = –3, φ = 0.2, and Re = 30

Table 4. Numerical values of the skin friction coefficient for different values of Re and solid volume fraction for three types of nanoparticle and α = 5°

Re	φ = 0	φ = 0.1			φ = 0.2		
		Cu	Al_2O_3	TiO_2	Cu	Al_2O_3	TiO_2
10	–0.181931	–0.228015	–0.236812	–0.236316	–0.302882	–0.321325	–0.319488
30	–0.0488096	–0.0547215	–0.0635752	–0.0630751	–0.070249	–0.0879484	–0.0869483
50	–0.0221866	–0.020245	–0.028929	–0.0284339	–0.0241233	–0.0414192	–0.0404258

Table 5. Numerical values of the Nusselt number (αNu) for different values of Re and solid volume fraction for three types of nanoparticles when α = 5° and Ec = 0.4

Re	φ = 0.1			φ = 0.2		
	Cu	Al_2O_3	TiO_2	Cu	Al_2O_3	TiO_2
10	4.11857	4.1796	4.17611	5.50722	5.6292	5.62211
30	3.77626	3.89544	3.88779	5.03454	5.27055	5.25443
50	3.655	3.71269	3.7062	4.91475	5.0224	5.00677

The variation of skin friction coefficient and Nusselt number with Reynolds number in three types of nanoparticles for different solid volume fraction is given in tabs. 4 and 5, as well as figs. 13 and 14, respectively. As expected that in divergent channel, the skin friction coefficient c_f and Nusselt number decrease when the Reynolds number Re increases for three considered nanoparticles and viscous fluid (φ = 0). It is observed that the values of skin friction coefficient c_f and Nusselt number for Al_2O_3 nanoparticles are larger than the other nanoparticles. Moreover, an increase in the skin friction coefficient and Nusselt number is observed when solid volume fraction increases. For water-Al_2O_3 nanofluid and φ = 1, the skin friction coefficient and Nusselt number for different values of the Reynolds number and angle α is presented in tab. 6. This table shows that in divergent channel c_f and Nusselt number decrease when angle α increases in the divergent channel whereas there are increase in c_f and Nusselt number in convergent channel when the Reynolds number Re and angle α increase. On the other hand, the skin friction coefficient and Nusselt number are increasing function of the solid volume fraction of nanoparticles in both divergent and convergent channels.

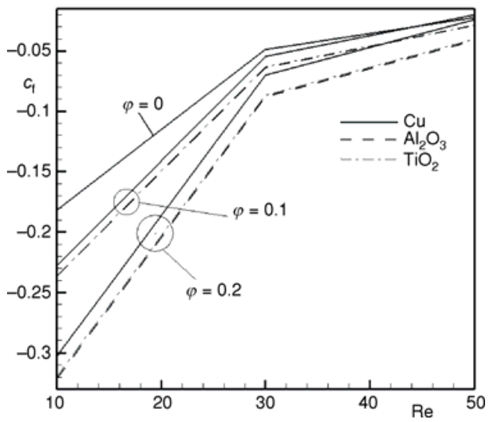

Figure 13. The variation of skin friction coefficient with Reynolds number in three types of nanoparticles for different solid volume fraction

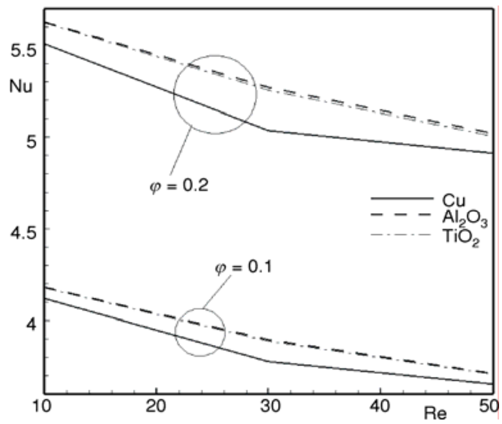

Figure 14. The variation of Nusselt number with Reynolds number in three types of nanoparticles for different solid volume fraction

Table 6. Numerical values of the skin friction coefficient and Nusselt number for different values of Re and α in divergent and convergent channel for water-Al_2O_3 nanofluid with φ = 0.1 and Ec = 0.6

Re	α	c_fRe	αNu	α	c_fRe	αNu
10	3	–1.89307	6.32394	–3	–2.10252	6.64549
20		–1.78733	6.17642		–2.20602	6.81748
30		–1.6811	6.03935		–2.30856	6.99567
40		–1.75452	5.91359		–2.41008	7.17914
30	2	–1.78838	6.16255	–2	–2.207	6.80261
	4	–1.57301	5.93255	–4	–2.40874	7.20064
	6	–1.35507	5.77202	–6	–2.60481	7.64386

The effects of nanoparticles on critical Reynolds number are also studied. As mentioned in many related textbooks and papers, in divergent channel, as Reynolds number increases, reverse flows in divergent channels emerge. Table 7 shows how nanoparticles affect on critical Reynolds number in the divergent channel for α = 5. It is clearly noticed that critical Reynolds number in divergent channel decreases for nanofluids. As shown in tab. 7, for Cu nanoparticles, separation occurs between Re = = 50 and Re = 60 when α = 5. While without considering nanoparticles (φ = 0), separation and backflow are observed around Re = 80. Further, Cu nanoparticle has lower critical Reynolds number rather than that of other nanoparticles. The effect of nanoparticles on the dimensionless velocity for water-TiO_2 nanofluid when φ = 0.1 and α = 5 is shown in fig. 15. It is observed that in divergent channel backflow is started after Re = 80.

Table 7. The effects of nanoparticles on critical Reynolds numbers in the divergent channel when α = 5

Re	$f'(1)$			
	φ = 0	φ = 0.1, Cu	φ = 01, TiO_2	φ = 0.1, Al_2O_3
50	–1.21026	–0.655705	–1.19394	–1.20157
60	–0.994799	0.249569	–0.96132	–0.97875
80	0.041216	0.5345	0.155357	0.13987
100	0.241266	0.89764	0.38545	0.36874

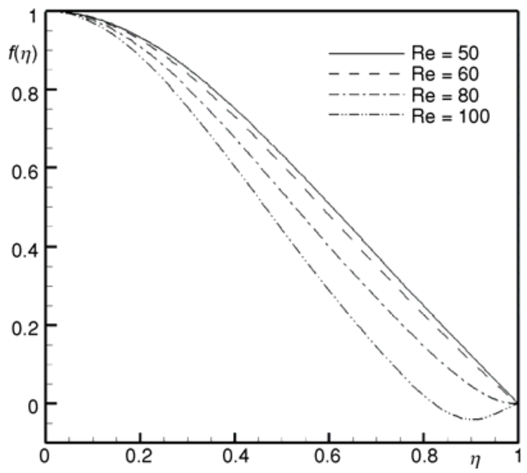

Figure 15. The effect of Reynolds number Re **on $f(\eta)$ for water-TiO_2 nanofluid when: φ = 0.1 and α = 5 in a divergent channel**

Conclusions

Analysis has been carried out for the influences of nanofluid and heat transfer effects on the flow quantities in convergent/divergent channel. Series solution for velocity and temperature are constructed by DTM. The present results of Newtonian fluid are compared with the other previous results [11, 52]. Numerical solution is also computed. A good agreement is noted between the results by different techniques. It is observed that the effects of material parameters of fluid on skin friction coefficient and Nusselt number are opposite for the convergent and divergent channels. Influences of Re and angle α on $f(\eta)$, $\xi(\eta)$, skin friction coefficient and Nusselt number in divergent and convergent channels are quite opposite. The effects of solid volume fraction on the skin friction coefficient and Nusselt number in convergent and divergent channels are similar. Interestingly, the water-Al_2O_3 nanofluid has higher values of skin friction coefficient c_f and Nusselt number when compared with the other two nanofluids.

Acknowledgment

This paper was funded by the Deanship of Scientific Research (DSR), King Abdulaziz University (KAU), under grant no. 10-130/1433HiCi. The authors, therefore, acknowledge technical and financial support of KAU.

Nomenclature

c_f – skin friction coefficient, (= τ_w/fU^2), [–]
c_p – specific heat at constant pressure, [JKg^{-1}K^{-1}]
Ec – Eckert number (μc_p/k$_0$), [–]
F – transformed function, [–]
G – transformed function [-]
k – thermal conductivity, [Wm^{-1}K^{-1}]
Nu – Nusselt number (= $rq_w|_{\theta=\alpha}/k_0T_w$), [–]
p – pressure, [Nm^{-2}]
Pr – Prandtl number (= U^2/c_pT_w), [–]
Re – Reynolds number (= $rU\alpha/\nu$), [–]
r – radial co-ordinate [m]
T – temperature [K]
u – radial velocity [ms^{-1}]
V – flow velocity vector [ms^{-1}]
y – analytic function, [–]
Y – transformed function, [–]

Greek symbols

α – angle between two unparallel walls, [deg]
η – similarity variable (= θ/α), [–]
Θ – transformed function, [–]
θ – angular co-ordinate, [deg]
μ – dynamic viscosity of fluid, [kgm^{-1}s^{-1}]
ξ – dimensionless parameter, [–]
ρ – fluid density, [kgm^3]
τ – shear stress, [Nm^{-2}]

Subscripts

nf – nanofluid
r – radiation
w – wall

References

[1] Goldstein, S., Modern Developments in Fluid Mechanics, Oxford, UK, 1938
[2] Rosenhead, L., The Steady Two-Dimensional Radial Flow of Viscous Fluid between Two Inclined Plane Walls, *Proc. Roy. Soc A, 175* (1940), 963, pp. 436-467.
[3] Makinde, O. D., Effect of Arbitrary Magnetic Reynolds Number on MHD Flow in Convergent-Divergent Channels, *Int. J. Numer. Methods Heat Fluid Flow, 18* (2008), 6, pp. 697-707
[4] Reza, M. S., Channel entrance flow, Ph. D. thesis, Department of Mechanical Engineering , University of Western Ontario, 1997
[5] McAlpine, A., Drazin, P. G., On the Spatio-Temporal Development of Small Perturbations of Jeffery-Hamel Flows, *Fluid Dynamic Research*, *22* (1998), 3, pp. 123-138
[6] Ganji, Z. Z., *et al*., Study on Nonlinear Jeffery-Hamel Flow by He's Semi-Analytical Methods and Comparison with Numerical Results, *Comput. Math. Appl*., *58* (2009), 11-12, pp. 2107-2116
[7] Esmaili, Q., *et al*., An Approximation of the Analytical Solution of the Jeffery-Hamel Flow by Decomposition Method, *Phys. Letter A*, 372 (2008), 19, pp. 3434-3439
[8] Makinde, O. D., Mhone, P. Y., Hermite-Pade Approximation Approach to MHD Jeffery-Hamel Flows, *Appl. Math. Comput., 181* (2006), 2, pp. 966-972
[9] Domairy, G., *et al*., The Application of Homotopy Analysis Method to Solve Nonlinear Differential Equation Governing Jeffery-Hamel flow, *Comm. Nonlinear Sci. Numer. Simulat*., *14* (2008), 1, pp. 85-95
[10] Moghimia, S. M., *et al.,* Homotopy Perturbation Method for Nonlinear MHD Jeffery-Hamel Problem, *Comp with Mathematics with Application, 61* (2011), 8, pp. 2213-2216
[11] Motsa, S. S., *et al*., A New Spectral Homotopy Analysis Method for the MHD Jeffery-Hamel Flow Problem, *Computer and Fluids*, *39* (2010), 7, pp. 1219-1225
[12] Choi, S. U. S., Enhancing Thermal Conductivity of Fluids with Nanoparticle, *The Proceedings of the 1995 ASME International Mechanical Engineering Congress and Exposition*, San Francisco, USA, ASME, FED 231/MD 66 (1995), pp. 99–105.
[13] Das, S. K., *et al*., Nanofluids: Science and Technology, John Wiley and Sons Inc., New York, USA, 2007
[14] Chen, H., Ding, Y., Heat Transfer and Rheological Behavior of Nanofluids a Review, *Adv.Tranp. Phenomena 1* (2009), ed. By Liqiu Wang, Springer, pp. 135-177
[15] Abu-Nada, E., Application of Nanofluids for Heat Transfer Enhancement of Separated Flows Encountered in a Backward Facing Step, *Int. J. Heat Fluid Flow*, *29* (2008), 1, pp. 242-249
[16] Tiwari, R. J., Das, M. K., Heat Transfer Augmentation in a Two-Sided Lid-Driven Differentially Heated Square Cavity Utilizing Nanofluids, *Int. J. Heat Mass Transfer*, *50* (2007), 9-10, pp. 2002-2018
[17] Maïga, S.E. B., *et al*., Heat Transfer Enhancement by Using Nanofluids in Forced Convection Flows, *Int. J. Heat Fluid Flow, 26* (2005), 4, pp. 530-546
[18] Polidori, G., *et al*., A Note on Heat Transfer Modeling of Newtonian Nanofluids in Laminar Free Convection, *Int. J. Thermal Sci*., *46* (2007), 8, pp. 739-744

[19] Oztop, H. F., Abu-Nada, E., Numerical Study of Natural Convection in Partially Heated Rectangular Enclosures Filled with Nanofluids, *Int. J. Heat Fluid Flow*, *29* (2008), 5, pp. 1326-1336
[20] Nield, D. A., Kuznetsov, A. V., The Cheng- Minkowycz Problem for Natural Convective Boundary-Layer Flow in a Porous Medium Saturated by a Nanofluid, *Int. J. Heat Mass Transfer*, *52* (2009), 25-26, pp. 5792-5795
[21] Kuznetsov, A. V., Nield, D. A., Natural Convection Boundary Layer Flow of Nanofluid Past a Vertical Plate, *Int. J. Thermal Sci*., *49* (2010), 2, pp. 243-247
[22] Kuznetsov, A. V., Nield, D. A., Double-Diffusive Natural Convection of Boundary Layer Flow of Nanofluid Past a Vertical Plate, *Int. J. Thermal Sci*., *50* (2011), 5, pp. 712-717
[23] Nield, D. A., Kuznetsov, A. V., The Cheng- Minkowycz Problem for Double-Diffusive Natural Convection Boundary Layer Flow in a Porous Medium Saturated by a Nanofluid, *Int. J. Heat Mass Transfer*, *54* (2011), 1-3, pp. 374-378
[24] Izadi, M., *et al*., Numerical Study of Developing Laminar Forced Convection of a Nanofluid in an Annulus, *Int. J. Thermal Sci*., *48* (2009), 6, pp. 2119-2129
[25] Cheng, P., Minkowcyz, W. J., Free Convection About a Vertical Flat Plate Embedded in a Porous Medium with Application to Heat Transfer from a Dike, *J. Geophys. Res*., *82* (1977), 14, pp. 2040-2044
[26] Khan, W. A., Aziz, A., Natural Convection Flow of a Nanofluid Over a Vertical Plate with Uniform Surface Heat Flux, *Int. J. Thermal Sci*., *50* (2011), 7, pp. 1207-1214
[27] Mahmoodi, M., Numerical Simulation of Free Convection of Nanofluid in a Square Cavity with an Inside Heater, *Int. J. Thermal Sci*., *50* (2011), 11, pp. 2161-2175
[28] Hassani, M., *et al*., An Analytical Solution for Boundary Layer Flow of a Nanofluid Past a Stretching Sheet, *Int. J. Thermal Sci*., *50* (2011), 11, pp. 2256-2263
[29] Judy, J., *et al*., Characterization of Frictional Pressure Drop for Liquid Flows through Microchannels, *Int. J. Heat Mass Transfer*, *45* (2002), 17, pp. 3477-3489
[30] Tso, C. P., Mahulikar, S. P., Experimental Verification of the Role of Brinkman Number in Microchannels using Local Parameters, *Int. J. Heat Mass Transfer, 43* (2000), 10, pp. 1837-1849
[31] Morimi, G. L., Viscous Heating In Liquid Flows in Microchannels, *Int. J. Heat Mass Transfer, 48* (2005), 5, pp. 3637-3647
[32] Das, S. K., *et al*., Pool Boiling Characteristics of Nanofluids, *Int. J. Heat Mass Transfer, 46* (2003), 5, pp. 851-862
[33] Koo, J., Kleinstreuer, C., Laminar Nanofluid Flow in Micro-Heat Sinks, *Int. J. Heat Mass Transfer*, *48* (2005), 13, pp. 2652-2661
[34] Hady, F. M., *et al*., Radiation Effect on Viscous Flow of Nanofluid and Heat Transfer over a Nonlinearly Stretching Sheet, *Naoscale Res. Lett*., *7* (2012), 1, pp. 224-236
[35] Motsumi, T. G., Makinde, O. D., Effects of Thermal Radiation and Viscous Dissipation on Boundary Later Flow of Nanofluids over a Permeable Moving Flat Plate, *Phy. Scr*., *86* (2012), 4, 045003-0450010
[36] Hung, Y. M., Analytic Study on Forced Convection of Nanofluids with Viscous Dissipation in Microchannels, *Heat Transfer Eng*., *31* (2010), 14, pp. 1184-1192
[37] Kuznetsov, A. V., *et al*., Thermally Developing Forced Convection in a porous medium: Circular Duct with Walls at Constant Temperature, with Longitudinal Conduction and Viscous Dissipation Effects, *Trans. Porous Media*, *53* (2003), 3, pp. 331-345
[38] Nield, D. A., *et al*., Thermally Developing Forced Convection in a Porous Medium: Parallel Plate Channel with Walls at Uniform Temperature, with Axial Conduction and Viscous Dissipation Effects, *Int. J. Heat Mass Transfer*, *46* (2003), 4, pp. 343-351
[39] Nield, D. A., *et al*., Effects of Viscous Dissipation and Flow Work on Forced Convection in a Channel Filled by a Saturated Porous Medium, *Trans. Porous Media*, *56* (2004), pp. 351-367.
[40] Zhou, J. K., *Differential Transformation Method and Its Application for Electrical Circuits* (in Chinese), Hauzhang Univ. press, Wuhan, China, 1986
[41] Rashidi, M. M., Erfani, E., New Analytical Method for Solving Burgers' and Nonlinear Heat Transfer Equation and Comparison with HAM, *Comp. Phys. Commun.*, *180* (2009), 9, pp. 1539-1544
[42] Joneidi, A. A., *et al*., Differential Transformation Method to Determine Fin Efficiency of Convective straight Fins with Temperature Dependent Thermal Conductivity, *Int. Commun. Heat Mass Transfer, 36* (2009), 7, pp. 757-762
[43] Chang, S. H., Chang, I. L., A New Algorithm for Calculating One-Dimensional Differential Transformation of Nonlinear Functions, *Appl. Math. Comput*., *195* (2008), 2, pp. 799-808

[44] Chang, S. H., Chang, I. L., A New Algorithm for Calculating Two-Dimensional Differential Transformation of Nonlinear Functions, *Appl. Math. Comput*., *215* (2009), 7, pp. 2486-2494
[45] Jang, B., Solving Linear and Nonlinear Initial Value Problems by the Projected Differential Transform Method, *Comp. Phys. Commun*., *181* (2010), 5, pp. 848-854
[46] Rashidi, M. M., Erfani, E. A New Analytical Study of MHD Stagnation-Point Flow in Porous Medium with Heat Transfer, *Computer &Fluid, 40* (2011), 1, pp. 172-178
[47] Rashidi, M. M., The Modified Differential Method for Solving MHD Boundary-Layer Equations, *Comp. Phys. Commun*., *180* (2009), 11, pp. 2210-2217
[48] Chen, C. K., Ju, S. P., Application of Differential Transformation to Transient Advective Dispersive Transport Equation, *Appl. Math. Comput*., *155* (2004), 1, pp. 25-38
[49] Chen, C. K., Chen, S. S., Application of the Differential Transformation Method to a Non-Linear Conservative System, *Appl. Math. Comput.*, *154* (2004), 2, pp. 431-441
[50] Franco, A., An Analytic Method for the Optimum Thermal Design of Convective Longitudinal Fin Arrays, *Heat Mass Transfer, 45* (2009), 12, pp. 1503-1517
[51] Brinkman, H. C., The Viscosity of Concentrated Suspensions and Solutions, *J. Chem. Phys*., *20* (1952), 4, pp. 571-581
[52] Esmaeilpour, M., Ganji, D. D., Solution of Jeffery-Hamel Flow Problem by Optimal Homotopy Asymptotic Method, *Comp. Math. Appl*., *59* (2010), 11, pp. 3405-3411

Paper submitted: April, 10, 2012
Paper revised: August 8, 2012
Paper accepted: November 19, 2012